High-resolution optical coherence tomography over a large depth range with an axicon lens

Zhihua Ding, Hongwu Ren, Yonghua Zhao, J. Stuart Nelson, and Zhongping Chen

Beckman Laser Institute and Center for Biomedical Engineering, University of California, Irvine, Irvine, California 92612

In optical coherence tomography, axial and lateral resolutions are determined by the source coherence length and the numerical aperture of the sampling lens, respectively. Whereas axial resolution can be improved by use of a broadband light source, there is a trade-off between lateral resolution and focusing depth when conventional optical elements are used. We report on the incorporation of an axicon lens into the sample arm of an interferometer to overcome this limitation. Using an axicon lens with a top angle of 160°, we maintained 10-μm or better lateral resolution over a focusing depth of at least 6 mm. In addition to having high lateral resolution, the focusing spot has an intensity that is approximately constant over a greater depth range than when a conventional lens is used. © 2002 Optical Society of America

OCIS codes: 170.4500, 110.0110.

Three-dimensional high-resolution optical imaging has potential clinical applications in the emerging field of biomedical optics. In a conventional optical imaging system, axial and lateral resolutions are correlated; hence one cannot obtain both in the same system. Optical coherence tomography (OCT) is a new modality that provides high-resolution sub-surface microstructural images in a noninvasive manner.[1,2] OCT uses coherence gating to select minimum backscattered photons for image reconstruction. Axial and lateral resolutions are determined by the source coherence length and the numerical aperture of the sampling lens, respectively. Whereas axial resolution can be improved by use of a broadband light source,[3,4] there is a trade-off between lateral resolution and focusing depth when conventional optical elements (spherical lenses, mirrors, etc.) are used, because a beam cannot be produced that has simultaneously a long focal depth and a narrow lateral width. Whereas high-lateral-resolution imaging requires a large numerical aperture, a long focal depth requires a small numerical aperture. In high-speed OCT imaging, in which an axial scanning mode (A mode) is used, a tightly focused lens produces a micrometer-sized spot at only one specific depth. The coherence gate quickly moves out of the shallow depth of focus during the scan. Although dynamic focusing compensation[3–5] can be used to overcome this limitation, one can use this method only at low speeds and therefore only in low-frame-rate OCT systems. In addition, dynamic focusing lenses are bulky and cannot be used when physical space is limited, such as in endoscopic OCT.[6,7]

We incorporated an axicon lens[8] into the sample arm of an interferometer to achieve both high lateral resolution and a greater depth of focus simultaneously. The term "axicon" was introduced by McLeod[8] to describe an optical element that produces a line image lying along the axis from a point source of light. There are many different kinds of axicon (rings, cylinders, etc.), but the single refracting cone lens is the most common form. Hence here we refer to an axicon lens as meaning specifically a refracting conical lens. Using an axi-

con lens with a top angle of 160°, we maintained 10-μm or better lateral resolution over a focusing depth of at least 6 mm. In addition to having high lateral resolution, the focusing spot has an intensity that is approximately constant over a greater depth range.

A high-speed phase-resolved OCT system at 1.3 μm is used in our experiments. A detailed system design has already been described in the literature.[9] We incorporate an axicon lens into the sample arm of the interferometer. A schematic of the interferometer with a fused-silica axicon lens (2.54-cm diameter, top angle of 160°; 1050−1350-nm antireflection coating, 3-mm edge thickness, and a diffraction index of 1.44681 at 1.3-μm wavelength) is shown in Fig. 1.

Light emitted from a single-mode fiber is collimated with a lens to produce spatially coherent illumination upon the axicon lens. Spatially coherent illumination is necessary if the axicon lens is to produce a coherent and sharply focused spot, similarly to a conventional lens. If spatially incoherent light illumination is used, the spot becomes wider and spatially incoherent,[10] resulting in reduced transverse resolution and a low signal-to-noise ratio in OCT. The intensity distribution,
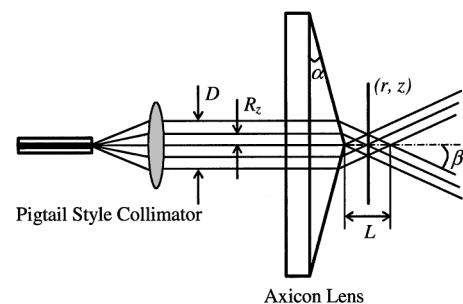

Fig. 1. Schematic of the sample arm of the OCT system with an axicon lens to achieve simultaneous high lateral resolution and greater depth of focus: α, angle formed by the conical surface with the flat surface of the axicon lens; β, intersection angle of the geometrical rays with the optical axis; R_z, radius of the incident beam; D, waist of the incident beam; L, depth of focus.

© 2002 Optical Society of America

$I(r, z)$, behind the axicon lens illuminated by a collimated beam of diameter D is given by[11]

$$I(r,z) = E^2(R_z)R_z \frac{2\pi k \sin \beta}{\cos^2 \beta} J_0{}^2(kr \sin \beta),$$
$$R \leq D/2, \qquad z \leq L, \quad (1)$$

where $E^2(R_z)$ is the energy of the incident beam at radius R_z that contributes to the intensity at axial point z through the relationship

$$R_z = \frac{z \tan \beta}{1 - \tan \alpha \tan \beta}, \qquad (2)$$

where k is the wave number, J_0 is a zero-order Bessel function of the first kind, r is a radial coordinate on the observation plane, and L is the depth of focus, approximated by

$$L = \frac{D(\tan^{-1} \beta - \tan \alpha)}{2}, \qquad (3)$$

where $\beta = \sin^{-1}(n \sin \alpha) - \alpha$. The angle of intersection of geometrical rays with the optical axis is deduced from Snell's law and takes the form

$$n \sin \alpha = \sin(\alpha + \beta), \qquad (4)$$

where n is the refractive index of the axicon lens and α is the angle formed by the conical surface with the flat surface of the axicon lens. According to Eq. (1), central peak radius ρ_0 of the beam behind the axicon lens can be predicted by the first zero of the Bessel function:

$$J_0(k\rho_0 \sin \beta) = 0, \qquad (5)$$

to result in

$$\rho_0 = 2.4048\lambda/2\pi \sin \beta. \qquad (6)$$

Inserting the parameters that pertain to the axicon lens ($\alpha = 10°$, $D = 2$ mm, $\lambda = 1.3$ μm, and $n = 1.44681$) into Eqs. (3) and (6) yields an estimated depth of focus L of 12.4 mm and a central peak radius ρ_0 of 6.32 μm.

To test our OCT system's performance we measured the relation of the detected signal to the mirror's axial position behind the axicon lens by blocking out the reference arm and using a reflecting mirror as the sample (Fig. 2). For comparison, the ratio of the signal to the axial position of a conventional lens ($f = 10$ mm; NA, 0.35 was also measured. The result clearly demonstrates that the axicon lens has a much greater focusing range than the conventional lens. The focusing range is approximately 7 mm (full width at $1/e^2$), which is smaller than the theoretical value of 12 mm. The reason for the reduced focusing range is that the spherical geometrical shape of the axicon's apex acts as an equivalent lens and focuses the central part of the illuminating light to a point away from the axicon's apex. Because focal energy with an axicon lens is distributed along the focusing range, the power

at each focusing point for an axicon lens is smaller than that for a conventional focusing lens. In Fig. 2 the detected peak signal ratio of the conventional to the axicon lens is ~16. There is a compromise between signal intensity and focusing range. However, our current system, which uses an over-the-counter axicon lens, has a focusing range of more than 6 mm. If an axicon lens designed specifically for OCT is made with a focusing range of 2 mm, the difference in peak intensity between the axicon and conventional lenses will be further reduced.

The focusing range and lateral resolution of the axicon-lens-based OCT system was calibrated with a variable-frequency resolution target from Edmund Scientific (Barrington, N.J.) Sequences of OCT images were made with targets located at different axial positions. The density of the parallel bar to be imaged was 50 line pairs/mm, which corresponds to a spatial
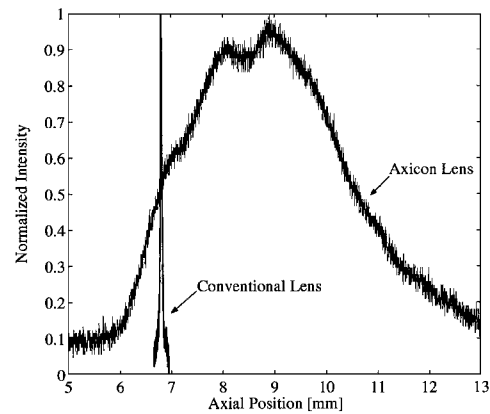

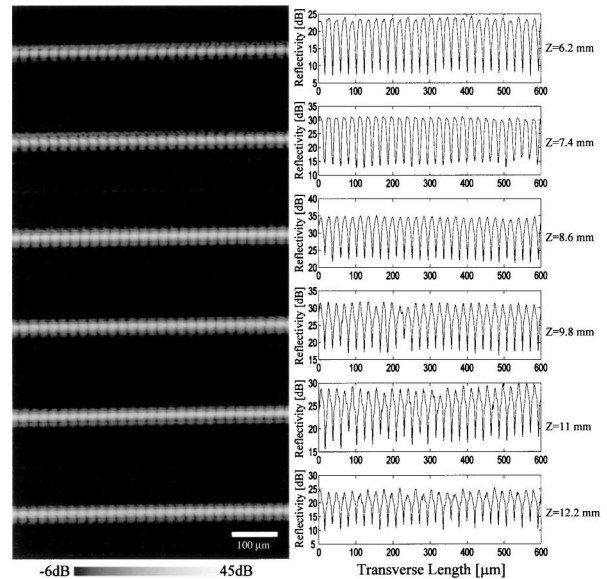Fig. 2. Signal versus axial position in the sample arm of the interferometer.

Fig. 3. OCT images and their cross-sectional profiles normal to the bar direction (noise floor, −6 dB). Images are successive from top to bottom and show a target located at different axial positions relative to the axicon apex at intervals of 1.2 mm over a total observed depth of 6 mm.
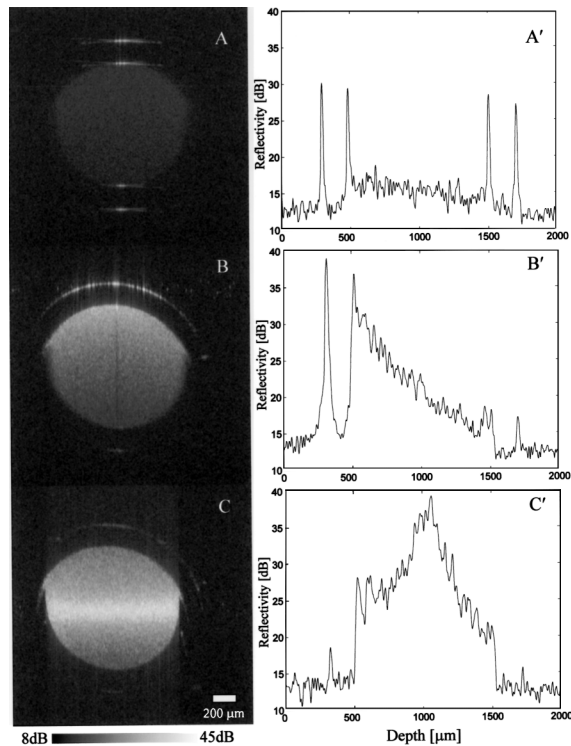
Fig. 4. OCT images of a capillary tube with polystyrene microspheres and their profiles along the center of the tube in depth directions that correspond to different focusing conditions in the sample arm: A, A′ axicon lens; B, B′; conventional lens focusing at the top of the tube; C, C′, conventional lens focusing at the center of the tube.

resolution of 10 μm. Figure 3 shows the OCT images and their corresponding cross-sectional profiles for the target located at different axial positions relative to the axicon apex with an interval of 1.2 mm over a total observed depth of 6 mm. The OCT image size was 600 μm by 200 μm. These results confirm a focusing depth range of at least 6 mm with 10-μm or better lateral resolution. In contrast, the Rayleigh range for a TEM_{00} Gaussian beam with a 10-μm waist radius at a wavelength of 1.3 μm was less than 0.25 mm.

To confirm the feasibility of the axicon-lens-based OCT system, we took images of the same sample with both axicon and conventional lenses. The sample comprised polystyrene microspheres (diameter, 0.356 μm) inside a capillary tube immersed in water. The internal diameter of the tube was 1.1 mm, and the wall thickness was 0.20 mm. The 2.7% polystyrene microsphere solution was diluted with distilled water at a volume ratio of 1:10 (scattering coefficient calculated to be 4.8 cm^{-1}). An OCT image with an axicon lens is shown in Fig. 4A, where both the lumen and the tube wall can be observed; image size is 2 mm by 2 mm. An OCT signal as a function of depth plotted across the center of the lumen is shown in Fig. 4A′. Although a slow decay in the signal is observed as a function of depth, this decay is due mainly to scattering at-

tenuation by the microspheres. For comparison, OCT images with a conventional lens at different focusing positions in the lumen are shown in Figs. 4B and 4C. The bright regions correspond to the focusing depths of the lens. Plots of the corresponding signals as a function of depth (Figs. 4B′ and 4C′) compared with those in Fig. 4A′ clearly indicate that the signals strongly depend on the focusing locations of the lens. The OCT signal decayed much faster farther away from the focusing location. Thus, in addition to having high lateral resolution over a greater depth range, the OCT signal was more uniform over the depth range when an axicon lens was used.

In conclusion, we have achieved 10-μm or better lateral resolution over a focusing depth of at least 6 mm by using an axicon lens with a top angle of 160° in our OCT system. These results demonstrate that an axicon lens can be used in an OCT system to maintain high lateral resolution over a greater depth of field, which is essential for high-resolution, high-speed OCT.

References

1. D. Huang, E. A. Swanson, C. P. Lin, J. S. Schuman, W. G. Stinson, W. Chang, M. R. Hee, T. Flotte, K. Gregory, C. A. Puliafito, and J. G. Fujimoto, Science **254,** 1178 (1991).
2. Z. Chen, Y. Zhao, S. M. Srinivas, J. S. Nelson, N. Prakash, and R. D. Frostig, IEEE J. Sel. Top. Quantum Electron. **5,** 1134 (1999).
3. W. Drexler, U. Morgner, F. X. Körtner, C. Pitris, S. A. Boppart, X. D. Li, E. P. Ippen, and J. G. Fujimoto, Opt. Lett. **24,** 1221 (1999).
4. I. Hartl, X. D. Li, C. Chudoba, R. K. Ghanta, T. H. Ko, J. G. Fujimoto, J. K. Ranka, and R. S. Windeler, Opt. Lett. **26,** 608 (2001).
5. Z. Chen, T. E. Milner, D. Dave, and J. S. Nelson, Opt. Lett. **22,** 64 (1997).
6. G. J. Tearney, S. A. Boppart, B. E. Bouma, M. E. Brezinski, N. J. Weissman, J. F. Southern, and J. G. Fujimoto, Opt. Lett. **21,** 543 (1996).
7. A. M. Rollins, R. U.-Arunyawee, A. Chak, C. K. Wong, K. Kobayashi, M. V. Sivak, and J. A. Izatt, Opt. Lett. **24,** 1358 (1999).
8. J. H. McLeod, J. Opt. Soc. Am. **44,** 592 (1954).
9. Y. Zhao, Z. Chen, C. Saxer, S. Xiang, J. F. de Boer, and J. S. Nelson, Opt. Lett. **25,** 114 (2000).
10. A. T. Friberg and S. Y. Popov, Appl. Opt. **35,** 3039 (1996).
11. R. M. Herman and T. A. Wiggins, J. Opt. Soc. Am. A **8,** 932 (1991).